International Journal of Engineering and Information Systems (IJEAIS)
ISSN: 2643-640X
Vol. 3 Issue 10, October – 2019, Pages: 27-39

Energy Management Based on Hierarchical Structure of an Isolated Microgrid Using Grasshoppers Optimization Algorithm

Ahmed H. Elmetwaly*
Electrical power and Machines department
The higher Institute of Engineering, El'Shorouk Academy
Cairo, Egypt
eng.ahmedhussain7@gmail.com

Azza A. Eldessouky
Electrical power and Machines department
Faculty of Engineering,
Port-Said University, Egypt

Abdelhay A. Sallam
Electrical power and Machines department
Faculty of Engineering,
Port-Said University, Egypt

***Abstract*—** *Microgrids (MGs) have been widely spreaded for its many benefits as they improve reliability and resilience of electrical grids, manage the addition of distributed energy resources (DERs) like wind and solar photovoltaic (PV) generation to reduce fossil fuel emissions, and provide electricity in areas not served. This study presents an adaptive scheme based on hierarchical system structure for energy management for an isolating MG. The proposed energy management system has been developed to manage the utilization of power among the hybrid energy resources, battery energy storage system (BESS) and Fuel cell (FC) based on Grasshoppers optimization algorithm (GOA) with an objective function including maintenance and emission cost for Diesel generator (DG) and microturbine generator (MT). Case study is presented including different loads. The optimization is aimed at minimizing the cost function of the system while constraining it to meet the customer demand and safety of the systems.*

Keywords—Microgrids (MGs), Photovoltaic (PV), Wind energy system (WES), Battery energy storage (BESS), Grasshopper optimization algorithm (GOA)

1. INTRODUCTION

MGs are electricity distribution systems containing loads and DERs that can be operated in a controlled, coordinated way while connected to the main power network or operated in an isolated mode. Energy management aspects are measure issues in MGs. Optimal management of electrical power in MG can significantly contribute in achieving the required economical operation. The management of the MG units require an accurate economic model to describe the operating cost taking into account the output power produces. Such a model is discrete and nonlinear in nature; hence optimizations tools are needed to reduce the operating costs to a minimum level.

The MG central controller uses the information from local electrical and thermal needs, power quality requirement, electricity and fuel costs, emission reduction, etc. to compute the amount of the power that should be taken from the main utility. In [1-5] a hierarchical control had managed the overall system operation using a dedicated Microgrid central supervisory controller (MCC) to achieve objectives such as minimizing operation cost, the emissions due to (NOx or CO_2 or SO_2), in addition to maximizing the system reliability. The MCC in the hierarchical structure could easily integrate objectives as well as operational constraints in a central optimization problem [6, 7]. Also, it can easily integrate various types of (DERs), real-time electricity price signals, thermal system, etc. The load and renewable forecasts can be used to further improve the system economics. The MCC system usually requires a dedicated powerful computer to solve the optimization problem in real time. Communication and control system redundancy is required to maintain a high reliability of the information and communication technology (ICT) system.

This paper introduces firstly, an energy management system based on control system for an isolated MG including PV and wind energy system (WES) as primary sources while, the BESS and the proton exchange membrane fuel cell (PEMFC) are acting as secondary sources. Moreover, the diesel and MT generators are acting as backup generators to meet the load demand. The main contributions of this work can be summarizing as:

1- An adaptive scheme based on hierarchical system for energy management for an isolating MG including different DERs is introduced.

2- In order to keep frequency within acceptable ranges, the optimal power among the hybrid resources, BESS, FC based on GOA with an objective function including maintenance and emission cost is presented.

3- Three operation modes covering all situations of the isolated MG with case study are presented.

The outlines of this paper are given as follows. In the next section, the architecture of MG is illustrated. In Section 3 is presented the proposed strategy algorithm. In Section 4, the simulation results of the proposed energy management strategy. Finally, the conclusion is presented in Section 5.

2. ISOLATED MG ARCHITECTURE

First, with a hierarchical control system, the MCC coordinates the aggregated operation of the DERs and loads. Each of these DERs is connected with local controller (LC) and is responsible for their reliable and economical operation, as well as interaction with the main grid uses the information from local electrical, power quality requirement, electricity and fuel costs and emission reduction. The main tasks of the MCC are summarized as:

- Providing the individual power and voltage set point for each power flow/micro source controller.
- Ensuring that the electrical loads are satisfied.
- Minimizing emissions and system losses.
- Maximizing the operational efficiency of the DERs.
- Providing logic and control for islanding and reconnecting the MG during events

The proposed MG includes PV, WES, BESS and PEMFC each of these resources is connected with local controller (LC) and the all sources are connected with MCC. The LC is consisting of breaker for switching operation of each resources and maximum power point tracking (MPPT) circuit. Fig. 1 shows the isolated MG with a hierarchical system structure.

2.1 Mathematical model of the PV

The power output of the PV generator, P_{PV} , can be calculated according to the following equation [10]:

$$P_{pv} = \eta_g N_{pv} A_m G_t \tag{1}$$

Where η_g is the instantaneous PV generator efficiency, A_m is the area of a single module used in a system (m^2), G_t is the global irradiance incident on the titled plane (w/m^2), and N_{PV} is the number of modules. The instantaneous PV generator efficiency is represented as [8]:

$$\eta_g = \eta_r \eta_{pt} [1 - \beta_t (T_c - T_r)] \tag{2}$$

Where η_r is the PV generator reference efficiency, η_{pt} the efficiency of power tracking equipment, which is equal to 1 if a perfect maximum power point tracker is used, T_c the temperature of PV cell in °C, T_r the PV cell reference temperature and t β_t is the temperature coefficient of efficiency.

The artificial neural network (ANN) [9] is used to predict the required voltage for obtaining MPP. This voltage is used to calculate the desired duty cycle of the boost converter. The ANN consists of three layers. The input layer has 2 neurons corresponds to the irradiation and temperature), the hidden Layer has 10 neurons while the output Layer has one. The maximum number of epochs to train the ANN equals 100 and the learning rate equals 0.02. The parameters of the PV model used in this paper are adjusted according to a real PV module (KC200GT) manufactured by KYOCERA [10] and are shown in table A.1 (Appendix A). The local controller of PV system is designed for extracting power when: $0 \leq T \leq 60$ & $100 \leq G_t \leq 1000$.

2.2 Mathematical model of the WES

The power output from wind turbine generator can be calculated as [11]:

$$\begin{cases} Pw = 0 & V < V_{ci} \\ Pw = aV^3 - bP_r & V_{ci} < V < V_r \\ Pw = P_r & V_r < V < V_{co} \\ Pw = 0 & V > V_{co} \end{cases} \tag{3}$$

Where $a = \frac{P_r}{(V_r^3 - V_{ci}^3)}$, $b = \frac{V_{ci}^3}{(V_r^3 - V_{ci}^3)}$, P_r is the rated power, V_{ci},, Vco and V_r are the cut-in, cut-out and rated speeds of the wind turbine. Actual power available from wind turbine is given by:

$$P_w = \frac{1}{2}\,\rho A C_p(\lambda,\beta)\left[\frac{Rw_{opt}}{\lambda_{opt}}\right]^3 \quad (4)$$

where ρ is the air density (ρ = 1.225 kg/m3), R is the blade length, A is swept area of the blade, w_{opt} is the optimum speed of wind turbine and λ_{opt} is the optimum tip-speed ratio. The power coefficient C_p depends on the pitch angle β and the tip speed ratio λ and is given by:

$$\lambda = \frac{\omega R}{V_w} \quad (5)$$

where ω is the rotational speed of the wind turbine and generator and V_w is the wind speed. The MPPT is obtained using perturbation and observation (P&O) [12]. The WES specifications are shown in Table A.2.

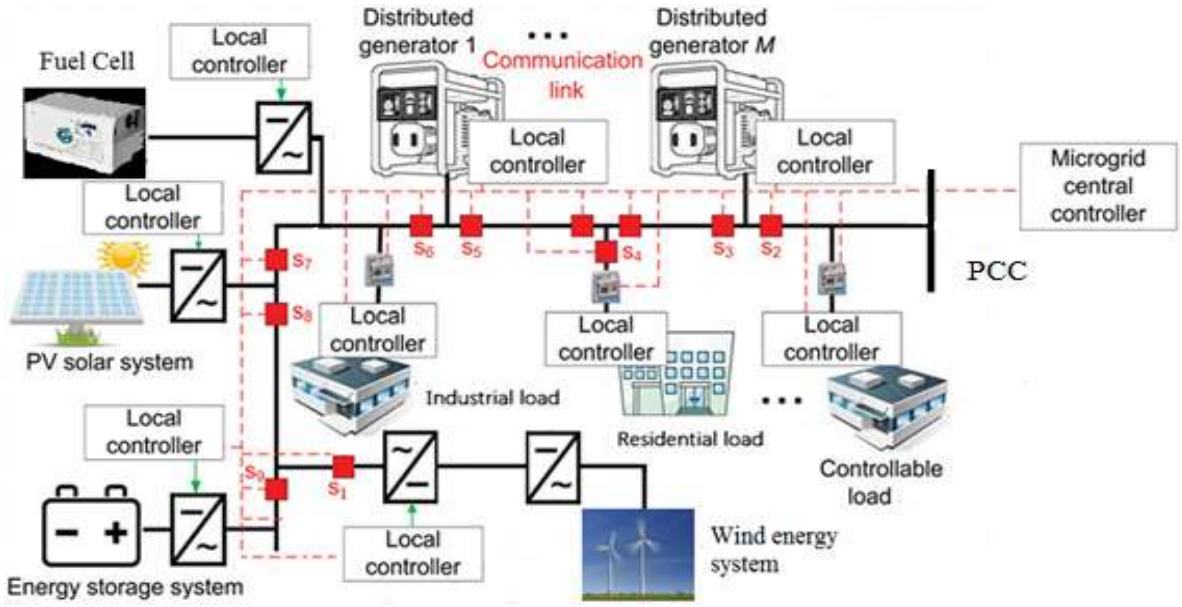

Fig. 1. *Diagram of an isolated MG with a control system structure.*

2.3 Mathematical model of the BESS

The battery bank, which is usually of the lead-acid type, is used to store surplus electrical energy or in discharging state. In case when the supplying power at hour *t* can be described by [13]:

$$C_{bat} = C_{bat}(t-1)(1-\sigma) \pm \left[\frac{E_{load}(t)}{\eta_{inv}} - (E_{pv}(t) + E_W(t))\right]\eta_{bat} \quad (6)$$

On the other hand, when the load demand is greater than the available energy generated, the battery bank is in discharging state. Therefore, the available battery bank capacity at hour *t* can be expressed using equation (6) but in subtraction sign.

Where $C_{bat}(t)$, $C_{bat}(t-1)$: The available battery bank capacity (wh) at hour (t) and ($t-1$) Respectively;

η_{bat}: The battery efficiency;

σ : The self-discharge rate of the battery bank;

$E_{PV}(t)$, $E_W(t)$: The energy generated by PV, wind generators respectively;

$E_{load}(t)$: The load demands in MG at hour t and

η_{inv} : The converter efficiency

The objective of the battery local controller is to charge and discharge the battery according to available renewable source power, state of charge (SOC) and load demand. The SOC of the battery is given by [14]:

$$SoC = SoC_0 + \int_{t0}^{t} \left(\frac{I_{bat}}{Cap_{bat}}\right) dt \tag{7}$$

where Cap_{bat} is battery capacity (Ah) and I_{bat} is the battery current (A). The BESS parameter is shown in Table A.3.

2.4 Mathematical model of the PEMFC

A FC is an electrochemical device that combines hydrogen and oxygen to produce electricity, with water and heat as its by-product. Due to the performance characteristics of the PEMFC such as fast start-up, light weight, high power density, and low operating temperature, the PEMFC is the most popular type of FCs and the best candidate for residential and vehicular applications. The fuel to PEMFC has been provided by the hydrogen tank which has been designed to store the hydrogen produced by the electrolyser. The electrolyser in turn gets its input from the dc bus. The FC parameters such as open circuit voltage (E_{oc}), the exchange current (I_c) and the Tafel slope (A) are depend on variations in temperature, pressures, compositions and flow rates of fuel and air. Therefore, to calculate the FC parameters, the following formulas are used [15]

$$V_{fc} = \left(E_{oc} - NA\ln\left(\frac{I_{fc}}{I_c}\right) * \frac{1}{s\frac{T_d}{3}+1}\right) - RI_{fc} \tag{8}$$

Where:

$$E_{oc} = K_c E_n \tag{9}$$

$$I_c = \left(\frac{zFk(P_{H_2}+P_{O_2})}{Rh}\right) e^{\left(\frac{-\Delta G}{KT}\right)} \tag{10}$$

$$A = \frac{RT}{Z\alpha F} \tag{11}$$

where K_c is voltage constant at nominal condition of operation, E_n is Nernst voltage, which is the thermodynamics voltage of the cells and depends on the temperature and partial pressure of reactants and products inside the stack (V), R is universal gas constant (8.3145 J/(mol K)), F is Faraday's constant (96485 A s/mol), Z is number of moving electrons, α is charge transfer coefficient, T is operating temperature (K), P_{H_2} is partial pressure of hydrogen inside the stack (atm), P_{O_2} is partial pressure of oxygen inside the stack (atm), k is Boltzmann's constant (1.38×10^{-23} J/K), h = Planck's constant (6.626×10^{-34} J s), and ΔG is size of the activation barrier which depends on the type of electrode and catalyst used. The local controller of the PEMFC is designed for extracting power when: $Pressure \geq 4$ bar. The parameters of FC are shown in Table A.4.

2.5 The Load LC (LLC)

The practical load data is given from Hurghada city in Egypt which consists of two parts. These are residential (Pres) and industrial (Pind) load as shown in Fig. 2.

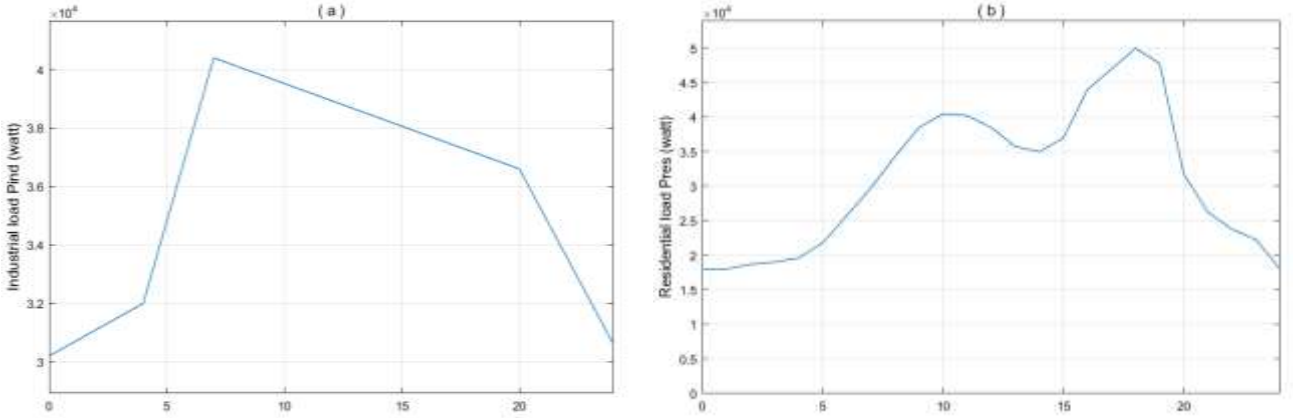

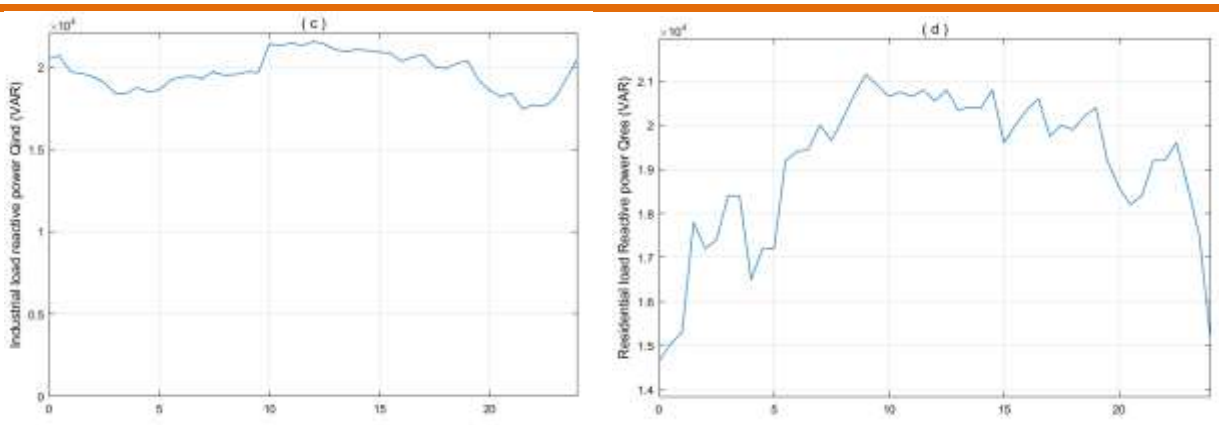

Fig. 2. *The load profile curve of (a) industrial load active power (P_{ind}), (b) residential load active power (P_{res}), (c) industrial load reactive power (Q_{ind}), (d) residential load reactive power (Qres).*

2.6 Case Study Data

In order to validate the proposed strategy algorithm, a case study of our research of Hurghada in Egypt at latitude of 27.225°, longitude at 33.791° is selected as this place consists of variable loads. Then, the irradiation and wind speed at this place from date 01/01/2018 to 31/12/2018 are collected assisted by web site SODA [16]. The table below shows the average monthly irradiation and wind speed of the selected case study.

Table 5: the average monthly irradiation and wind speed of the selected case study.

Month	Irradiation (W/m^2)	Wind Speed (m/sec)
January	278.5	4.15
February	340.1	2.48
March	395.5	3.45
April	435.8	4.9
May	473.2	3.62
June	472.3	5.96
July	465.6	6.34
August	442.2	6.56
September	386.3	7.27
October	335.2	4.78
November	273.3	3.77
December	254.2	4.85

3. THE PROPOSED STRATEGY ALGORITM

The algorithm of MCC is shown in fig. 3. From which there are three operation modes for the selected case study.

- *Operation mode#1:* **w**hen all loads (P_{ind}+P_{res}) covered by the DERs power (P_{PV} +Pw).so the surplus power is used to charge the BESS and controllable loads if founded.
- *Operation mode#2:* When the total loads power is more than the DERs power, so the BESS power (P_{bat}) and the FC extracted power (P_{fc}) is covering the deficit power.
- *Operation mode#3: (the Worst case):* If all DERs power (P_{PV} +Pw), BESS power (P_{bat}) and FC power (P_{fc}) can't provide enough power to the load or one of DERs sources be cut off. In this case, the GOA is employed to economically dispatch power between different DER sources, the diesel generator (DG) and MT in order to economically satisfy the deficit load

power demand, while taking into account the environmental externality costs by minimizing the emissions of nitrogen oxides (NOx), sulfur oxides (SO_2), and carbon oxides (CO_2). Comparing the work presented herein with those of other method [19] for

energy management, the GOA with an objective including emission, maintenance and operation costs of MT and DG is studied. The objective function is expressed as

$$CF = \sum_{i=1}^{N}(C_i F_i + OM_i) + \sum_{i=1}^{N}\sum_{j=1}^{M}\alpha_j(EF_{ij}P_i) \quad (12)$$

Where:

C_i & F_i : The fuel cost & consumption rate of generation unit *I*, respectively.

OM_i : The operation and maintenance cost of a generating unit *i*.

α_j : The externality cost of emission type j.

EF_{ij} : The emission factor of generating unit, emission type j.

N : The number of generation unit.

M : Emission types (NOx or CO_2 or SO_2)

The operating and maintenance costs OM are assumed to be proportional with the produced energy, where the proportionally constant is K_{OMi} for unit *i*.

$$OM_i = K_{OMi}\sum_{i=1}^{N} P_i \quad (13)$$

Where the values of the K_{OM} for DG and MT equal 0.01258 and 0.00587 $ / kWh, respectively. The externality costs and emission factors of the DG, and MT used in this study are summarized in Table A.6

The objective function should satisfy different constraints.

- Power balance constraints:

$$\sum_{i=1}^{N} P_i - (P_{res} + P_{ind}) + \left(P_{pv} + P_w + P_{fc} - P_{elz}\right) \pm P_{bat} = 0 \quad (14)$$

where P_{res} is the total power demand in *kW*, and P_{elz} is the electrolyzer consumption power.

- Generation capacity constraints

$$P_i^{min} \le P_i \le P_i^{max}, i = 1,2,\dots N \quad (15)$$

Where P_i^{min} & P_i^{max} are the minimum & the maximum operating power of unit *i*.

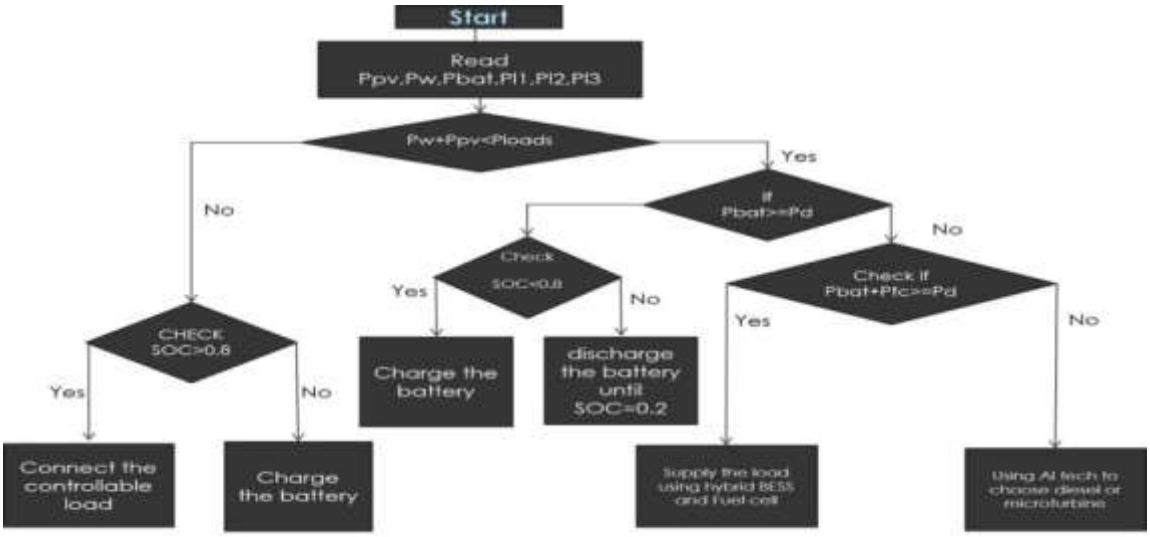

Fig. 3. *the algorithm of the central supervisory control*

According to statistics and the odds of each occurrence of each operation modes are shown in Table 6

Table 6: the statistics of each operation mode

Opertion mode	No. of days	Percentage of occurance
Opertion mode#1	126	34.52%
Opertion mode#2	153	41.91%
Opertion mode#3	81	22.19%

3.1 Implementation of the GOA

GOA is a recently proposed single objective, population based heuristic algorithm, which imitates the behavior of Grasshopper Swarms in nature and models it mathematically to solve optimization problems with contentious variables [18-19]. The algorithm simulates repulsion and attraction forces between Grasshoppers. While repulsion forces permit Grasshoppers to explore the search space, attraction forces urge them to exploit the promising regions. GOA was equipped with a coefficient, which decreases the comfort zone of the grasshoppers to balance exploration and exploitation phases over the course of optimization. This helps GOA not to become trapped in local optima and find a precise estimate of the global optimum. Since the best solution obtained so far by the swarm considered as a target to be chased, grasshoppers have a great chance to find the global optimum via improving the target over the course of iterations. The position updating equation of GOA is given as

$$X_i^d = r\left(\sum_{\substack{j=1 \\ j\neq i}}^{N} r\frac{ub_d - lb_d}{2} S\left(\left|X_j^d - X_i^d\right|\right)\frac{X_j - X_i}{d_{ij}}\right) + T_d \tag{16}$$

Where, X_i^d is the current solution's position in *d*-th dimension, *r* is a diminishing coefficient, which narrows the comfort, repulsion and attraction zones. the ub_d & lb_d are the upper & lower bounds in *d*-th dimension, *S* is a function, which defines the social forces between grasshoppers, d_{ij} is the absolute value of the distance between *j*-th grasshopper (X_j) and *i*-th grasshopper (X_i) and T_d is the target value in *d*-th dimension, which is the best solution found so far.

Eq. (16) shows that the next position of a grasshopper depends on its current position, the position of all other grasshoppers, and the position of the target. The social forces function in (16) is defined as:

$$S = fe^{\frac{-d}{l}} - e^{-d} \tag{17}$$

Where, *f* shows the strength of attraction and *l* is the attractive length scale. The parameter *r* in (16) is required to be decreased in proportion to the number of iterations to balance exploration and exploitation. This encourages exploitation as the iteration count increases. This parameter also reduces the comfort zone in proportion to the number of iterations and is calculated as

$$r = r_{max} - t\,\frac{r_{max} - r_{min}}{T} \tag{18}$$

Where r_{max} & r_{min} are the maximum & minimum values and are taken as 1 and 0.0004 in this work, *t* indicates the current iteration, and *T* is the maximum number of iterations.

The GOA parameters used to verify the performance of the GOA-PID controller are:

Number of search agents: 25

Number of iterations :20

The proposed implementation of the GOA procedure for determining the controller parameters and finding the global minimum error is illustrated in Fig. 4.

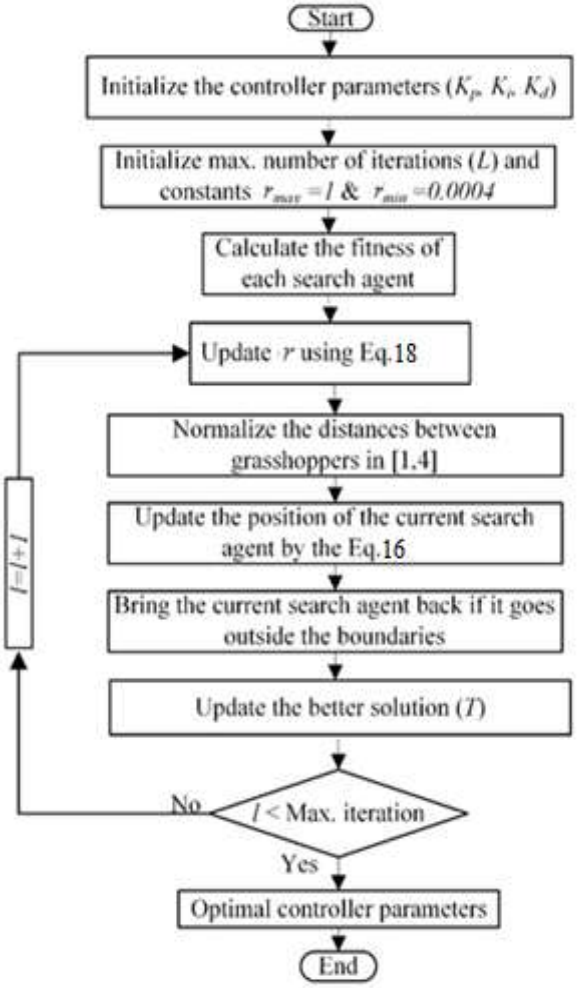

Fig. 4. *The proposed implementation of GOA procedure for determining controller parameter*

4. SIMULATION RESULTS

The proposed strategy algorithm has been simulated in MATLAB/Simulink platform. For observing the behavior of proposed algorithm with changing environmental and load conditions, two sets of environmental input data obtained during three days with different weather conditions in Hurghada region, Egypt. For operation mode #1, the day 29/6/2018 is selected when high wind speed and radiation were occurred. While, the day 25/12/2018 had medium wind speed and irradiation so it is determined for operation mode #2. Finally, for operation mode #3, a day 5/2/2018 in which low wind speed and irradiation was found is chosen.

Figs. 5(a)&(d) represents the variation of wind speed and its corresponding output power for operation mode #1. While, the irradiation of the PV and the corresponding output power are represented in fig.5(b) & (c), respectively. According to the irradiation, the PV LC controls the breaker of the PV to get opened when irradiation is out of range. Fig. 5 (e) &(f)) represents Pind and Pres. The MCC is taken a decision to charge the battery and/or hydrogen generation depending on the diffence power (P_{diff}) between the generated and load power. It is remarked that the value of P_{diff} is positive most of the times and the surplus power is used to charge the battery as shown in fig. 5(g).

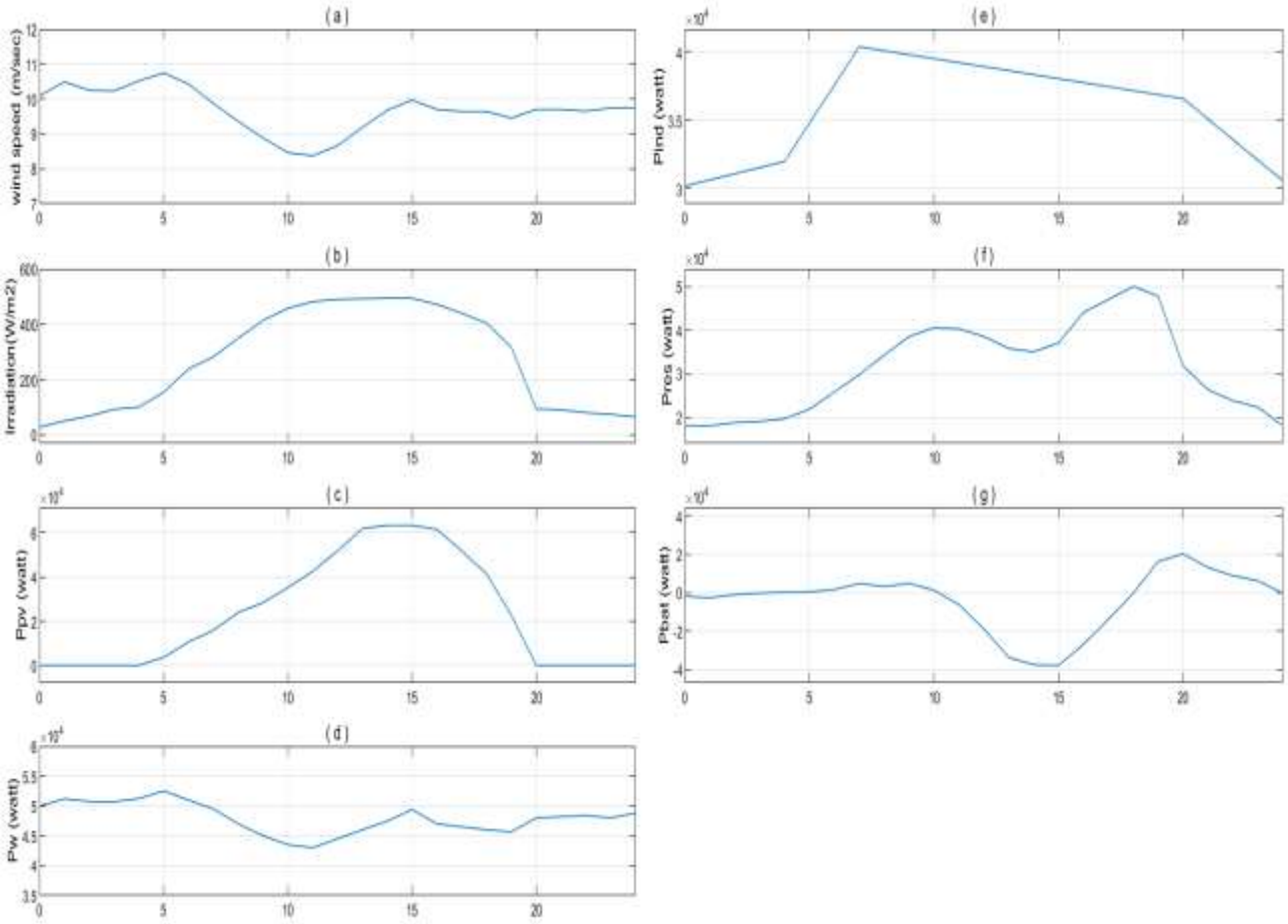

Fig. 5. *Simulation results of operation mode #1*

In case of operation mode #2, the selected day had moderate values of wind speed and PV irradiation. Therefore, the PEMFC is expected to be used during the period when the generation power from the DERs sources is less than the load power demand. Hence the electrolyser is operated to generate hydrogen to provide the required power to cover the deficit of load as shown in fig. 6(h). It is observed that the average wind speed was between 2 to 6 m/s. So, the P_w was lesser than its full capacity. Then breaker was opened and WES was isolated from 9 am to 12 pm. From fig. 6 (g), it is observed that the battery is getting charged for most of time and discharged for less duration.

The wind speed and PV irradiation are very low in case of operation mode #3. So, the breaker of the wind and PV is opened most hours of the day. The PEMFC is working and the BESS is discharged until reach the maximum value of discharge (20 kw) to cover the load. The deficiency of the power is compensated from MTs or DG according to the economic dispatch based on GOA as shown in fig. 7.

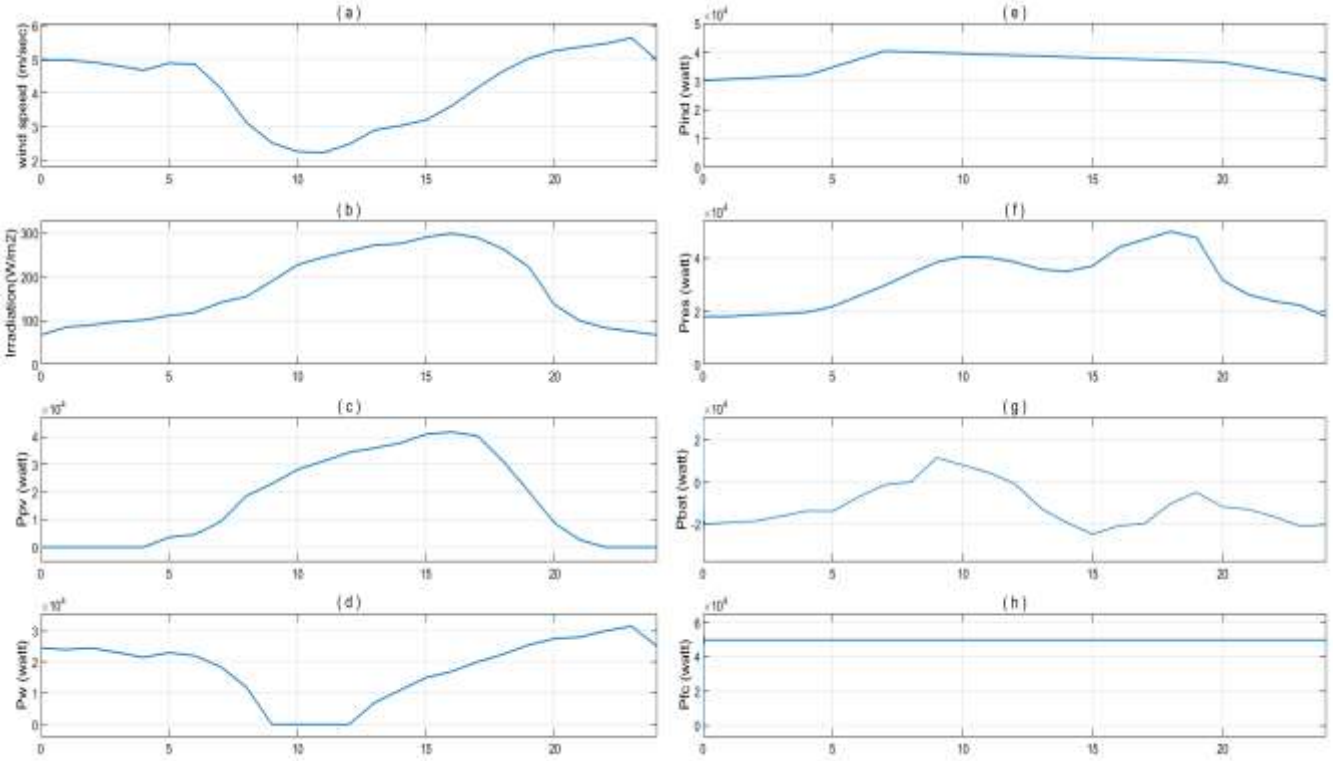

Fig. 6. *Simulation results of operation mode #2*

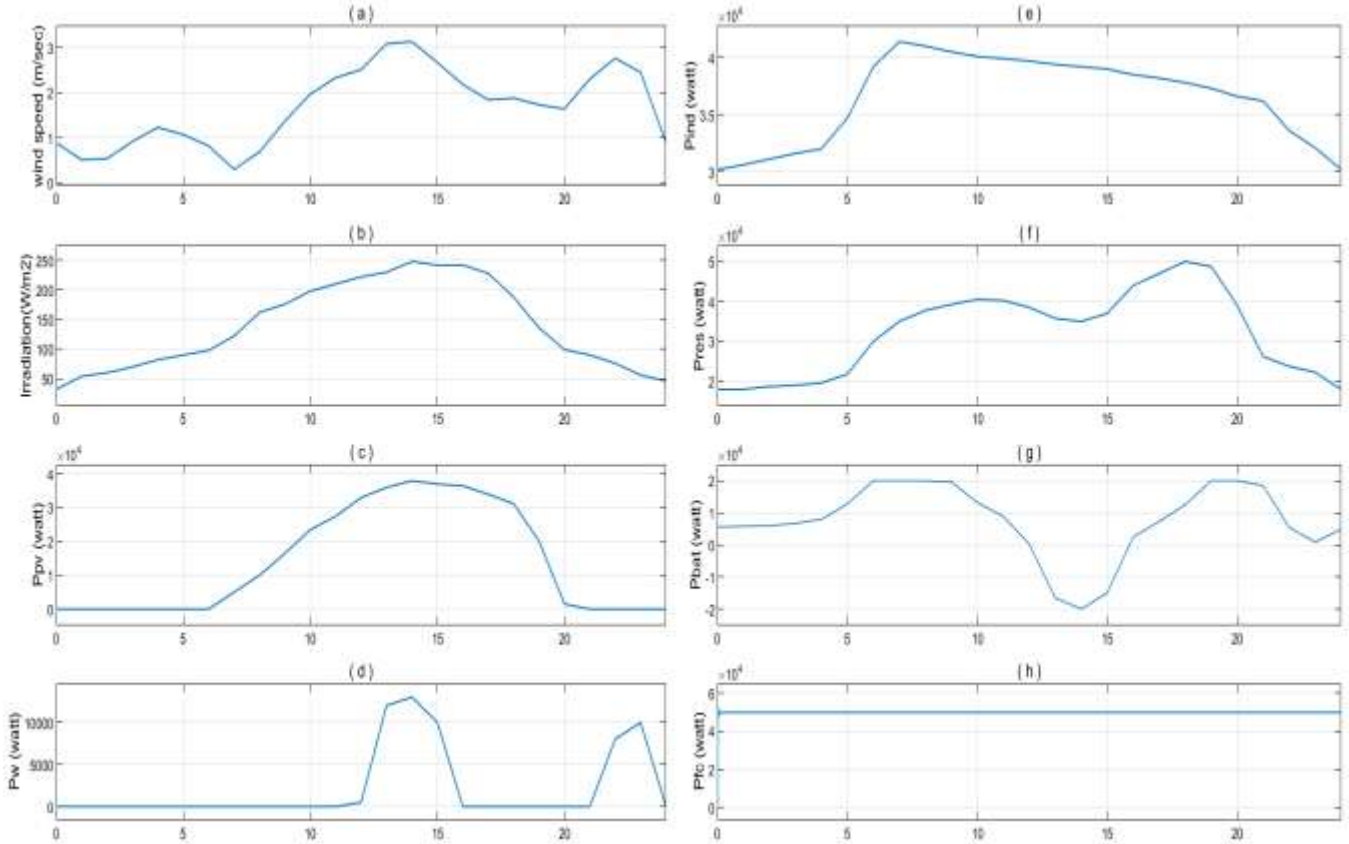

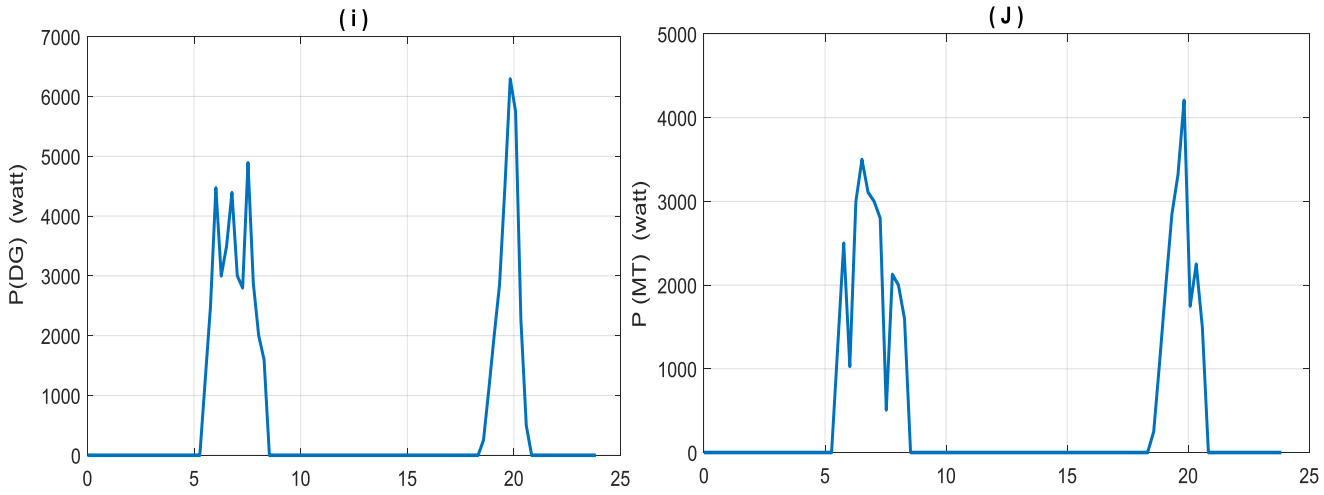

Fig. 7. *Simualtion results of operation mode #3*

5. CONCLUSION

An adaptive scheme based on a hierarchical system has been presented for energy management for an isolating MG. A new optimization technique based on GOA in order to optimally dispatch the electrical power among different DERs sources, BESS, FC, MT and DG is introduced. The results show the robustness of the proposed method to keep the balance between the generation and loads under different meteorological conditions and consequently the frequency is within acceptable ranges.

Appendix A

Table A.1: The Parameters of the PV module

Open circuit voltage (V_{OC})	Short circuit current (I_{SC})	Module voltage at maximum power point	Module current at maximum power point (I_m)	Maximum Power (Pm) of a PV module	Reference temperature	Reference solar radiation	No. of series PV modules in a string	No. of parallel connected PV strings
32.9 V	8.21 A	26.3 V	7.61 A	200W	25°C	1000W/m^2	8	63

Table A.2: Wind generations specification

Power rated (KW)	Vci (m/s)	Vco (m/s)	Vr (m/s)	Hub Height (m)	Swept Area (m^2)
60	2.5	16	12	16	140.235

Table A.3: Parameters of BESS

Capacity (Ah)	Efficiency (%)	Minimum charge (%)	Maximum charge (%)	Maximum discharging rate	Maximum charging rate
2160	85	20	80	20 kW	-40 kW

Table A.4: Parameters of FC

Type	Stake Nominal power	Nernst Voltage (E_n)	Fuel cell resistance
PEM	50 kW	1.1342 V	0.66404 Ω

Table A.5: the emission cost for DG and MT

Emission Type	Externality Costs $/Kg	Emission Factors for DG Kg/MWh	Emission Factor for MT Kg/MWh
NO_X	4.2	21.8	0.44
SO_2	0.99	0.454	0.008
CO_2	0.014	1.432	1.596

REFERENCES

[1] Lopes, J. A. P., Moreira, C. L., and Madureira, A. G. (2006). Defining control strategies for Microgrids islanded operation. IEEE Trans. Power Syst., Vol. 21, No. 2, pp. 916–924.

[2] Madureira, A., Moreira, C., and Lopes, J. A. P. (2005). Secondary load-frequency control for microgrids in islanded operation. Proc. International Conference on Renewable Energy and Power Quality, Zaragoza, Spain, pp. 1–4.

[3] Mehrizi-Sani, A., and Iravani, R. (2010). Potential-function based control of a microgrid in islanded and grid-connected modes. IEEE Trans. Power Syst., Vol. 25, No. 4, pp. 1883–1891.

[4] Arcidiacono, V., Menis, R., and Sulligoi, G. (2007). Improving power quality in all electric ships using a voltage and VAR integrated regulator. Proc. IEEE Electric Ship Technologies Symposium, Arlington, pp. 322–327.

[5] Arcidiacono, V., Castellan, S., Menis, R., and Sulligoi, G. (2006). Integrated voltage and reactive power control for all electric ship power systems. Proc. International Symposium on Power Electronics, Electrical Drives, Automation and Motion, Taormina, Italy, May, pp. 878–882.

[6] Yang, F., Feng, X., Oudalov, A., Li, Z., and Wang, Z. (2013). Microgrid energy management system and method for controlling operation of a microgrid. patent application number US 13/955,575.

[7] Zadeh, M. R. D., Hajimiragha, A., and Krok, M. J. (2012). Power generation optimization in microgrid including renewable power source. patent application number US. 13/358,487.

[8] M.G. Villalva, J.R. Gazoli and E. Ruppert F. (2009). Comprehensive Approach to Modeling and Simulation of Photovoltaic Arrays". IEEE Transactions on power electronics. Vol.24, NO. 5.

[9] Abdessamia Elgharbi, Dhafer Mezghani, Abdelkader Mami. (2012). A Maximum Power Point Tracking Method Based on Artificial Neural Network for PV System" International Journal of Advances in Engineering & Technology, Vol. 5, Issue 1, pp. 130-140**.**

[10] KYOCERA high efficiency photovoltaic module data sheet.

[11] Felix A. Farret, M. Godoy Simoes. (2006). Integration of alternative sources of energy. IEEE Press, Wiley-Interscience, John Wiley & Sons, INC.

[12] Abdullah, M. A., Yatim, A. H. M., Tan, C. W., & Saidur, R. (2012). A review of maximum power point tracking algorithms for wind energy systems. Renewable and Sustainable Energy Reviews, 16(5), 3220–3227. doi: 10.1016/j.rser.2012.02.016.

[13] S. Diaf, D. Diaf, M. Belhamel, M. Haddadi, A. Louche. (2007). A methodology for optimal sizing of autonomous hybrid PV/wind system. ScienceDirect, Energy Policy, Volume 35, Issue 11, pp. 5708-5718.

[14] Zhang, C.P.; Jiang, J.C.; Zhang, W.G.; Suleiman, M.S. (2012). Estimation of state of charge of lithium-ion batteries used in HEV using robust extended Kalman filtering. Energies, 5, 10981–11115.

[15] Natsheh. E, Natsheh. A and Albarbar. A. (2013). Intelligent controller for managing power flow within standalone hybrid power systems. IET Sci. Meas. Technol. 7(4): 191–200.

[16] http://www.soda-pro.com/web-services

[17] Xianyong Feng, Aditya Shekhar, Fang Yang, Robert E. Hebner & Pavol Bauerv. (2017). Comparison of Hierarchical Control and Distributed Control for Microgrid. Electric Power Components and Systems, 45:10, 1043-1056.

[18] Topaz CM, Bernoff AJ, Logan S, Toolson W. (2008). A model for rolling swarms of lo- custs. Eur Phys J Special Top; 157:93–109.

[19] T. Jumani, M. Mustafa, M. Rasid, N. Mirjat, M. Baloch, and S. Salisu. (2019). Optimal Power Flow Controller for Grid-Connected Microgrids using Grasshopper Optimization Algorithm. *Electronics*, vol. 8, no. 1, p. 111.